AFRL-RX-WP-JA-2017-0340

GREEN'S FUNCTION-BASED DEFECT IDENTIFICATION IN InAs-$InAs_{1-X}Sb_X$ STRAINED LAYER SUPERLATTICES (POSTPRINT)

S. Krishnamurthy

SRI International

Zhi Gang Yu

Washington State University

18 April 2017
Interim Report

AIR FORCE RESEARCH LABORATORY
MATERIALS AND MANUFACTURING DIRECTORATE
WRIGHT-PATTERSON AIR FORCE BASE, OH 45433-7750
AIR FORCE MATERIEL COMMAND
UNITED STATES AIR FORCE

REPORT DOCUMENTATION PAGE

Form Approved
OMB No. 0704-0188

1. REPORT DATE *(DD-MM-YY)*	2. REPORT TYPE	3. DATES COVERED *(From - To)*
18 April 2017	Interim	11 September 2013 – 18 March 2017

4. TITLE AND SUBTITLE
GREEN'S FUNCTION-BASED DEFECT IDENTIFICATION IN InAs-$InAs_{1-X}Sb_X$ STRAINED LAYER SUPERLATTICES (POSTPRINT)

5a. CONTRACT NUMBER
FA8650-11-D-5800-0008

5b. GRANT NUMBER

5c. PROGRAM ELEMENT NUMBER
62102F

6. AUTHOR(S)
1) S. Krishnamurthy – SRI International
2) Zhi Gang Yu – Washington State University

5d. PROJECT NUMBER
4348

5e. TASK NUMBER 0008

5f. WORK UNIT NUMBER
X0TW

7. PERFORMING ORGANIZATION NAME(S) AND ADDRESS(ES)
1) SRI International, 333 Ravenswood Ave. Menlo Park, CA 94025
2) Washington State University 410 E Spokane Falls Blvd. Spokane, WA 99202

8. PERFORMING ORGANIZATION REPORT NUMBER
AFRL/RX
Wright Patterson Air Force Base
Dayton, OH 45433

9. SPONSORING/MONITORING AGENCY NAME(S) AND ADDRESS(ES)
Air Force Research Laboratory
Materials and Manufacturing Directorate
Wright-Patterson Air Force Base, OH 45433-7750
Air Force Materiel Command
United States Air Force

10. SPONSORING/MONITORING AGENCY ACRONYM(S)
AFRL/RXAN

11. SPONSORING/MONITORING AGENCY REPORT NUMBER(S)
AFRL-RX-WP-JA-2017-0340

12. DISTRIBUTION/AVAILABILITY STATEMENT
Distribution Statement A. Approved for public release: distribution unlimited.

13. SUPPLEMENTARY NOTES
PA Case Number: 88ABW-2017-1846; Clearance Date: 18 Apr 2017. This document contains color. Journal article published in AIP Advances), Vol. 7, 15 Jun 2017. © 2017 AIP Publishing. The U.S. Government is joint author of the work and has the right to use, modify, reproduce, release, perform, display, or disclose the work.
The final publication is available at http://dx.doi.org/10.1063/1.4989564

14. ABSTRACT *(Maximum 200 words)*
We have extended the recently developed approach that employs first-principles Hamiltonian, tight-binding Hamiltonian, and Green's function methods to study native point defect states in InAs/$InAs_{0.7}Sb_{0.3}$ strained layer superlattices (SLS) latticed matched to GaSb. Our calculations predict a defect level at 250 meV below the GaSb valance band edge, in agreement with values deduced recently from lifetime measurements and analysis [Aytac et al. Phys. Rev. Appl., 5, 054016 (2016)]. In addition, we identify the defect level to be arising from an In-vacancy in the InAsSb region of the superlattice. The formation energy calculations further indicate that In-vacancies are easier to form in both regions of the superlattice than in bulk InAs or in InAsSb alloy. Our results suggest that In-vacancy is the most damaging native defect that limits lifetimes InAs/ InAs/$InAs_{0.7}Sb_{0.3}$

15. SUBJECT TERMS
Hamiltonian; Green's function; InAs/$InAs_{0.7}Sb_{0.3;}$ strained layer superlattice (SLS); GaSb; In-vacancy; InAsSb alloy

16. SECURITY CLASSIFICATION OF:			17. LIMITATION OF ABSTRACT:	18. NUMBER OF PAGES	19a. NAME OF RESPONSIBLE PERSON (Monitor)
a. REPORT	b. ABSTRACT	c. THIS PAGE			Joseph Burns
Unclassified	Unclassified	Unclassified	SAR	8	19b. TELEPHONE NUMBER *(Include Area Code)* (937) 255-9594

AIP ADVANCES 7, 065310 (2017)

Green's function-based defect identification in InAs-InAs$_{1-x}$Sb$_x$ strained layer superlattices

S. Krishnamurthy[1,a] and Zhi Gang Yu[2]
[1]*Applied Optics Laboratory, SRI International, Menlo Park, California 94025, USA*
[2]*Applied Sciences Laboratory, Washington State University, Spokane, Washington 99202, USA*

(Received 21 April 2017; accepted 9 June 2017; published online 15 June 2017)

We have extended the recently developed approach that employs first-principles Hamiltonian, tight-binding Hamiltonian, and Green's function methods to study native point defect states in InAs/InAs$_{0.7}$Sb$_{0.3}$ strained layer superlattices (SLS) latticed matched to GaSb. Our calculations predict a defect level at 250 meV below the GaSb valance band edge, in agreement with values deduced recently from lifetime measurements and analysis [Aytac et al. Phys. Rev. Appl., 5, 054016 (2016)]. In addition, we identify the defect level to be arising from an In-vacancy in the InAsSb region of the superlattice. The formation energy calculations further indicate that In-vacancies are easier to form in both regions of the superlattice than in bulk InAs or in InAsSb alloy. Our results suggest that In-vacancy is the most damaging native defect that limits lifetimes InAs/InAs$_{0.7}$Sb$_{0.3}$. [http://dx.doi.org/10.1063/1.4989564]

The type II superlattice (T2SL) in which the valence band of one of the constituents lies above or near the conduction band of the other constituent can be designed to absorb electromagnetic (EM) radiation with energy much smaller than the band gap of constituent compounds. In addition, the associated flat bands, photon recycling, and high-quality molecular-beam-epitaxy growth may increase the Auger, radiative, and Shockley-Read-Hall (SRH) recombination lifetimes respectively and T2SL promise a performance far superior to HgCdTe-based photodiodes.[1] However, in spite of serious efforts for over three decades,[2–5] the SRH-limited lifetimes in type II strained layer superlattice (SLS) systems—such as the InAs-GaSb system—are only a few tens of ns.[6–8] The lifetimes in InAs-InAsSb SLS are demonstrably longer— 185 ns[9] in the long-wave infrared (LWIR) wavelength region to a few hundred ns[10,11] to a few μs[12,13] in the mid-wave infrared (MWIR) region of the EM band. However, even in this system, the measured lifetimes are interpreted to be limited by SRH mechanisms.[14–17] Systematic analysis yields some clues on the native point defect (NPD) level location in the gap, but the defect origin is still unknown. A better understanding could enable defect mitigation, which is required to improve the device performance to be competitive to HgCdTe photodiodes.

In this Letter, we extend our recently developed[18,19] method—a combination of first-principles Hamiltonian, tight-binding Hamiltonian, and Green's function (GF) methods—and calculate the defect levels and their origins in two recently[14] well-studied InAs/InAs$_{0.7}$Sb$_{0.3}$ SLS systems. The defect levels calculated here agree well with those interpreted from the measured lifetimes. In addition, we predict that In-vacancy in the InAsSb region of the SLS is responsible for those defect levels. Further first-principles calculations of defect formation energies indicate that In-vacancies form more easily in these SLS systems than either in bulk InAs or InAsSb.

The detailed description and application of our method to predict defect levels in InAs-GaSb SLSs were published elsewhere.[18,19] Briefly, in this method, we calculate the unperturbed Hamiltonian H^0 using long-range, but sp^3 local orbitals-based, hybrid pseudopotential tight binding (HPTB) method[20] and the defect potential ΔV from first principles using SIESTA,[21] also with sp^3 local basis.

[a]email: srini@sri.com

The averaging of interatomic interactions across the interface is chosen so that HPTB Hamiltonian consistently produces a band gap at 77 K in a number of SLS systems in fairly good agreement with measurements[22–24] and other calculations.[25,26] In our calculations, the effect of temperature appears only through the band gap of the underlying Hamiltonian.

To use this method for InAs-InAsSb alloy SLS, several improvements must be made. First, we have further used the band structure code to obtain 77 K band gap of several InAs-InAsSb SLS, as shown in Table I, in good agreement with recent measurements.[14] The GF method, which uses the defect potential from first principles and HPTB Hamiltonian for the band structure, is in general valid and does not require any modification to consider alloys. The HPTB Hamiltonian had been successfully used[27] to study alloys and predict accurate electronic and optical properties by using the virtual crystal approximation. In general, the defect potential from first-principles is a major hurdle in the study of defects in alloys, as it would require an unrealistically large unit cell to achieve a random distribution of constituent atoms with non-interacting defects. Even then, the supercell calculations of bandstructures will correspond to the periodic array of distributed atoms and defects. However, in our method, the first-principles method is used to obtain only the local potential around the defect and not the band structure. Since the defect potential does not change beyond the 2nd neighbor, a supercell containing the superlattice need not be large. However, to adequately model a random distribution, we choose supercells containing 1000 atoms. These supercells typically contain one unit cell in the superlattice direction and many unit cells in the plane. The anion sites in the $InAs_{1-x}Sb_x$ region of the unit cell is randomly occupied by As and Sb atoms, subject to the composition (x) constraint. We calculate the defect potentials by relaxing the atoms around the defect. We consider the NPDs, anion vacancy (V_a), anion antisite (a_c), cation vacancy (V_c), and cation antisite (c_a) in both InAs and InAsSb regions of the supercell. In the alloy region, we note that additional NPDs need to be studied because the cation (In) in the alloy can form an antisite by substituting either of the two anions (As and Sb) sites. Similarly, either of the anions can form a vacancy. For convenience, we denote the atoms in the InAs region as In_1 and As_1, in InAsSb region as In_2, As_2, and Sb. In our studies we evaluate the energy levels from 11 NPDs, namely, V_{In1}, As_{In1}, V_{As1}, In_{As1}, V_{In2}, As_{In2}, V_{As2}, In_{As2}, V_{Sb}, In_{Sb}, and Sb_{In2}. In the case of V_{In2} and As_{In2}, and Sb_{In2}, the defect location is chosen so that its nearest neighbor sites are occupied by the most likely combination of As and Sb atoms for the given alloy concentration. For example, for x=0.3, the most likely anion neighbor combination for the cation is 3 As atoms and 1 Sb atom. In our SIESTA calculations, we use the local density approximation (LDA) in the Ceperley-Alder parametrization. The LDA pseudopotentials are obtained from the SIESTA website and the energy cut-off is set 400 Ryd. The DM tolerance for the SCF is 10^{-3} and the force tolerance for geometry optimization is 0.02 eV/Ang. For bulk alloy systems in the absence of defects, the structures have a fixed lattice constant as in GaSb, which correspond to strained structures.

We then apply the extended method to alloy SLS systems, particularly those that have been grown and studied experimentally. A recent publication[14] described measurement of lifetimes and photoluminescence (PL) in 7 different InAs-InAsSb SLS designs, and a careful data analysis indicated that the same defect state, which was located at about 250 meV below the valance band of GaSb, limited the lifetime in all 7 designs studied. The origin of the defect could not be established in that study. We selected two designs with smaller unit cells (which can be studied more accurately with the 1000-atom supercell for ΔV calculations)—InAs (30.1 Å)-$InAs_{0.7}Sb_{0.3}$ (9.8 Å) and

TABLE I. Calculated band gap (E_g), energy at valence band edge (E_v) and conduction band edge (E_c) for various SLS systems. All energies are in eV. E_v and E_c are given in energy w.r.t. E_v of InSb.

Design Label	InAs (ML)/ $InAs_{1-x}Sb_x$ (ML)	x	E_v [eV]	E_c [eV]	E_g (Calc) [eV]	E_g (Ref. 14) [eV]
A	19/4	38	-0.381	-0.178	0.203	0.204
B	24/5	39	-0.345	-0.177	0.168	0.162
C	28/6	40	-0.316	-0.176	0.140	0.135
D	10/3	30	-0.462	-0.177	0.286	0.290
E	15/5	30	-0.413	-0.172	0.241	0.240
F	20/7	32	-0.356	-0.168	0.189	0.185
G	25/8	34	-0.329	-0.169	0.161	0.155

InAs (45.8 Å)-$InAs_{0.7}Sb_{0.3}$ (15.0 Å)—for defect level and formation energy studies. In our calculations of SLS lattice matched to GaSb, the designs correspond to InAs (10 ML)-$InAs_{0.7}Sb_{0.3}$ (3 ML) and InAs (15 ML)-$InAs_{0.7}Sb_{0.3}$ (5 ML), where a monolayer (ML) contains a layer of anion and a layer of cation in growth direction along the [100]. For brevity, they are further denoted as 10/3 SLS and 15/5 SLS. The in-plane lattice constant of SLS is matched to that of GaSb. For the calculation of band structures, the lattice constant in the growth direction is modified by the ratio of the elastic constants $-2C_{12}/C_{11}$. All term values in the TB Hamiltonian of GaSb and InAs are rigidly shifted so that the valence band edge (E_v) of bulk InSb, GaSb and InAs are respectively 0.0 eV, -0.03 eV and -0.60 eV.[28] Since the same term values are used in the construction of the SLS Hamiltonian, the E_v and conduction band edge (E_c) can be obtained in a common energy scale for all designs by diagonalizing the Hamiltonian at Brillouin zone center. The SLS structures, the band gap (E_g), E_v, and E_c, for various SLS systems are summarized in Table I. Note that the calculated band gaps are in good agreement with the measured values.

For the selected two SLS systems, the first-principles ΔV and the TB bandstructures of the SLS are used in GF, to calculate the defect energy (E_t) levels for various defects. The defects were placed farthest away from either of the interfaces. In the case of 10/3 SLS, the defects in the InAsSb region is placed in 2nd ML. The calculated values, referenced to the respective valence band edges of the SLS, are given Table II. All energies are in meV. For easier comparison of defect levels across the SLS designs (and consistent with convention[28]), the E_c, E_v, and E_t are referenced to the InSb valence band edge and are plotted in Figure 1 for (a) 15/5 SLS and (b) 10/3 SLS designs. Only the defect levels (short-dashes) between the valence band and the conduction band of the SLS are shown. To denote the origin of the defects, the conduction (dashed line) and valence band (dotted line) of the InAs and $InAs_{0.7}Sb_{0.3}$ alloy are shown. The dash-dotted line (red online) denotes the defect energy level deduced[14] to be near 250 meV below the E_v of GaSb, which is 280 meV below that of InSb. In the 15/5 SLS, there are no defects originating from InAs and all defect states arise from the alloy region. In 10/3, V_{In} in InAs is also present. Importantly, notice that the defect V_{In2} in the alloy region of *both* SLS designs has the same energy level of -280 meV as deduced by experiments. While the position of this level in the gap was predicted by analyzing the temperature-dependent lifetimes, our calculations predict the origin to be *In* vacancy in alloy region. If, for example, these designs can be grown in In-rich conditions, it might be possible to suppress the vacancy density and thus improve the lifetimes. Also, our calculations predicted several states in addition to V_{In2}. In the case of 10/3 SLS, the defect levels are farther away from -280 meV and likely will not affect the lifetime calculations. However, in the case of 15/5, the defect state from In_{Sb} (in the alloy region) is somewhat closer to -280 meV. The impact of those levels on the lifetimes can be evaluated only when the defect densities and the cross section are calculated; we have not attempted these calculations here.

Similar to our observation[19] in InAs-GaSb SLS systems, we found that the change in defect potential, ΔV, calculated at the defect and the neighbor sites in both SLS systems did not vary much from that in the constituent bulk/alloy materials. In the event that wave functions and the GF in SLS change little from the bulk values, the energy levels of defects in SLS can be correlated to those in the bulk systems.[19] Since the GF approach can be used to calculate the defect states even resonant in the bands, we obtained *all* defect states in both InAs and $InAs_{0.7}Sb_{0.3}$ alloy as shown in Figure 2. The valence band edge of InAs is at -0.6 eV[28], with a 77 K gap of 0.4 eV. The calculated valence band offset and the band gap of $InAs_{0.7}Sb_{0.3}$ alloy are consistent with previous estimations.[14,24]

TABLE II. Calculated defect energy levels, measured w.r.t. the respective valance band of 15/5 and 10/3 SLS (in meV).

InAs ML / $InAs_{0.7}Sb_{0.3}$ ML	V_{In1}	As_{In1}	V_{As1}	In_{As1}	V_{In2}	As_{In2}	V_{As2}	In_{As2}	V_{Sb}	In_{Sb}	Sb_{In2}
15/5	--	--	--	--	30, 98, 136, 178, 228	--	--	32, 68, 87	40	29, 99, 110	--
10/3	8, 29, 67	--	--	--	10, 103, 110, 188, 257	--	0.298	14, 58, 74	297	40, 90, 110	--

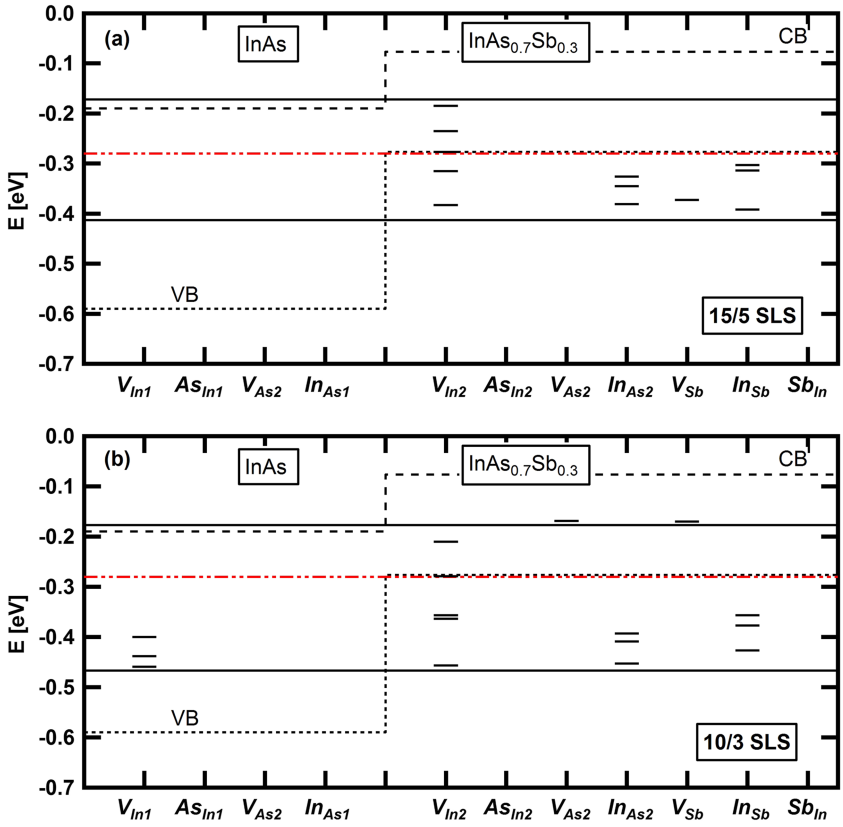

FIG. 1. Calculated defect levels (short dash) in the band gap of (a) 15/5 SLS and (b) 10/3 SLS. The conduction (dashed line) and valence band (dotted line) of constituent InAs and $InAs_{0.7}Sb_{0.3}$ alloy are shown. The conduction and valence band of SLS are shown by solid lines. The defect level predicted from Ref. 14 is shown by a dash-dotted line (red online). All energies are with respect to the InSb valence band edge.

Figure 2 shows the conduction band (short-dashed line), valence band (dotted line), and calculated bulk defect states (short-dashed line) in both InAs compound and $InAs_{0.7}Sb_{0.3}$ alloy. Superimposed on this band diagram are the lowest conduction and highest valence band of 15/5 SLS (thin-solid lines) and of 10/3 SLS (thick-dashed line). We see that defect levels of V_{In1}, V_{In2}, In_{As2}, and In_{Sb} are in the SLS gaps. By comparison, the full calculation of defect levels, displayed in Fig. 1a, also

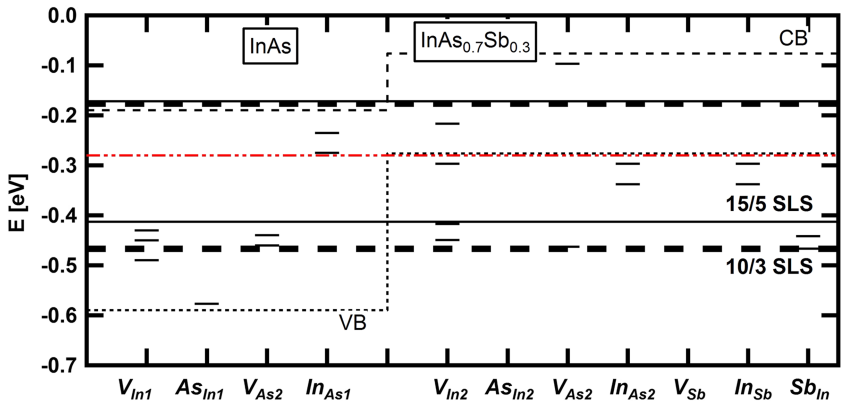

FIG. 2. Calculated bulk defect levels (short-dash), conduction band (dashed line), and valence band (dotted line) of InAs and $InAs_{0.7}Sb_{0.3}$ alloys are shown. The conduction and valence band of 15/5 SLS (thin line) and 10/3 SLS (thick short-dashed) are shown. The dash-dotted line (red online) denotes the defect level location predicted in Ref. 14.

TABLE III. Deviation of formation energy SLS NPDs from its bulk value in the respective compound/alloy (in eV).

InAs ML / $InAs_{0.7}Sb_{0.3}$ ML	V_{In1}	As_{In1}	V_{As1}	In_{As1}	V_{In2}	As_{In2}	V_{As2}	In_{As2}	V_{Sb}	In_{Sb}	Sb_{In2}
15/5	-0.16	-0.35	1.18	0.86	-1.11	-1.05	0.30	-0.59	-0.92	-1.09	-1.03
10/3	0.10	-0.09	1.43	1.20	-4.02	-2.02	-0.80	-1.15	-1.16	-1.02	-1.65

predicts these defects, except V_{In1}. A similar comparison between Fig. 2 and Fig. 1b indicates that the predicted defect set is common in both methods, except V_{In1} and V_{As1}. One-to-one correspondence between bulk defect states and SLS defect states can be expected only when each region is thick enough to likely have wavefunctions in the bulk region to be near-identical to that in bulk/alloy material. However, the simple design may be used to narrow down the list of likely defects prior to undertaking an expensive growth sequence.

We considered SLS only with abrupt interface. Although our calculations find (not reported here) that As_{Sb} and Sb_{As} defects do not produce any energy levels in the gap, we did not consider a large-scale inter-diffusion and its effect on the gap. The approach used here is ideally suited for more accurate calculations in which our HPTB Hamiltonian is replaced with a SIESTA Hamiltonian and hybrid functionals[29–31] to obtain a correct gap. That is, both ΔV and G^{0k} are calculated using the gap-corrected SIESTA Hamiltonian. However, those calculations are time consuming as they require a basis set considerably larger than sp^3 basis set[31] and extension of hybrid functionals to SLS has not been accomplished. Similarly, the GF method developed here can be used also to calculate the defect state wave function and hence the minority carrier lifetimes.[32] Those intensive calculations are useful only when the equilibrium defect density are evaluated.

It is important to note that our calculations predict the defect levels *if* the defects are present. The probability for any of these defects are not estimated. The likelihood of these defects being present depends on the defect formation energy (DFE). The DFE is the difference between the free energy of the final and initial states, and the final state free energy depends critically on the growth conditions. Hence the equilibrium calculations to obtain defect densities[33,34] are not attempted here. However, some trends can be established from the total (enthalpy) energy (E_{TOT}) calculations. The difference between [E_{TOT} (lattice with defect)-E_{TOT} (lattice without defect)]$_{SLS}$ and [E_{TOT} (lattice with defect)-E_{TOT} (lattice without defect)]$_{bulk}$ can suggest the trend in SLS with reference to the bulk constituents. E_{TOT} is the total energy calculated using first-principles with SIESTA, and details of the calculations is published elsewhere.[35] A negative (positive) value of this deviation energy from the bulk will indicate that the defect is more (less) likely to be present in the SLS, under growth conditions identical to that of the bulk. The calculated values for these designs are given in Table III. We note that V_{In2} is more likely to be present in both SLSs, further indicating that V_{In2} could be the defect observed in the experiments. A larger negative value for 10/3 is mainly because the defect is closer to the interface, and larger bond angle relaxation lowers the energy.

In summary, we have extended the hybrid method of the first-principles Hamiltonian, long-range empirical tight-binding Hamiltonian, and Green's function approaches to study NPDs in Ga-free alloy SLS structures. We have applied the method to two SLS structures recently grown and measured. Our detailed calculations agree with the conclusion that an energy level near -280 meV is present in both designs. However, we further pinpoint that the detrimental defect level originates from the In-vacancy in the alloy region of the SLS. The total energy calculations indicate that In-vacancy in SLS is more easily formed in SLS than in bulk. Growing those structures under In-rich conditions may reduce these damaging defects and lead to longer lifetimes.

The authors are grateful for funding from the United States Air Force (USAF Contract FA8650-11-D-5800/TO 0008) through a Universal Technology Corporation (UTC) subcontract (14-S7408-02-C1).

[1] C. H. Grein, J. Garland, and M. Flatte, J. Electron. Mater. **38**, 1900 (2009).
[2] D.-Y. Ting, Semiconductors and Semimetals **84**, 1 (2011).
[3] E. A. Plis, Adv. in Electronics **2014**, 246769.
[4] P. Martyniuk, J. Antoszewski, M. Martyniuk, L. Faraone, and A. Rogalski, Appl. Phys. Rev. **1**, 041102 (2014).

[5] A. Rogalski, Opto–Electron. Rev. **20**, 279 (2012).
[6] D. Rhiger, J. Electron. Mater. **40**, 1815 (2011).
[7] J. Pellegrino and R. DeWames, Proc. SPIE **7298**, 72981U (2009).
[8] D. Rhiger, R. E. Kvaas, S. F. Harris, and C. J. Hill, Infrared Physics & Technology **52**, 304 (2009).
[9] Y. Lin, D. Donetsky, D. Wang, D. Westerfeld, G. Kipshidze, L. Shterengas, W. L. Sarney, S. P. Svensson, and G. Belenky, J. Electron. Mater. **44**, 3360 (2015).
[10] E. H. Steenbergen, B. C. Connelly, G. D. Metcalfe, H. Shen, M. Wraback, D. Lubyshev, Y. Qiu, J. M. Fastenau, A. W. K. Liu, S. Elhamri, O. O. Cellek, and Y.-H. Zhang, Appl. Phys. Lett. **99**, 251110 (2011).
[11] D. Zuo, R. Liu, D. Wasserman, J. Mabon, Z.-Y. He, S. Liu, Y.-H. Zhang, E. A. Kadlec, B. V. Olson, and E. A. Shaner, Appl. Phys. Lett. **106**, 071107 (2015).
[12] B. V. Olson, E. A. Shaner, J. K. Kim, J. F. Klem, S. D. Hawkins, L. M. Murray, J. P. Prineas, M. E. Flatté, and T. F. Boggess, Appl. Phys. Lett. **101**, 092109 (2012).
[13] Y. Aytack, B. V. Olson, J. K. Kim, E. A. Shaner, S. D. Hawkins, J. F. Klem, M. E. Flatte, and T. F. Boggess, Appl. Phys. Lett. **105**, 022107 (2014).
[14] Y. Aytack, B. V. Olson, J. K. Kim, E. A. Shaner, S. D. Hawkins, J. F. Klem, M. E. Flatte, and T. F. Boggess, Phys. Rev. Appl. **5**, 054016 (2016).
[15] B. V. Olson, E. A. Shaner, J. K. Kim, J. F. Klem, S. D. Hawkins, M. E. Flatte, and T. F. Boggess, Appl. Phys. Lett. **103**, 052106 (2013).
[16] J. Wróbel, Ł. Ciura, M. Motyka, F. Szmulowicz, A. Kolek, A. Kowalewski, P. Moszczyński, M. Dyksik, P. Madejczyk, S. Krishna, and A. Rogalski, Semicond. Sci. Technol. **30**, 115004 (2015).
[17] B. Connelly, G. D. Metcalfe, H. Shen, M. Wraback, C. L. Canedy, I. Vurgaftman, J. S. Melinger, C. A. Affouda, E. M. Jackson, J. A. Nolde, J. R. Meyer, and E. H. Aifer, Journal of Electron. Mater. **42**, 3203 (2013).
[18] S. Krishnamurthy, D. van Orden, and Z.-G. Yu, J. of Electron. Mater. **45**, 4574 (2016).
[19] S. Krishnamurthy and Z.-G. Yu, Appl. Phys. Lett. **110**, 021113 (2017).
[20] A.-B. Chen and A. Sher, *Semiconductor Alloys* (Plenum, New York, 1995); Ch. 7.
[21] http://www.icmab.es/dmmis/leem/siesta/; see also, J. M. Soler, E. Artacho, J. D. Gale, A. García, J. Junquera, P. Ordejon, and D. Sanchez-Portal, J. Phys. Condens. Matter **14**, 2745 (2002).
[22] A. P. Ongstad, R. Kaspi, C. E. Moeller, M. L. Tilton, D. M. Gianardi, J. R. Chavez, and G. C. Dente, J. Appl. Phys. **89**, 2185 (2001).
[23] R. Kaspi, C. Moeller, A. Ongstad, M. L. Tilton, D. Gianardi, G. Dente, and P. Gopaladasu, Appl. Phys. Lett. **76**, 409 (2000).
[24] E. H. Steenbergen, O. O. Cellek, D. Lubyshev, Y. Qiu, J. M. Fastenau, A. W. K. Liu, and Y.-H. Zhang, Proc. SPIE **8268**, 82680K–1 (2012).
[25] F. Szmulowicz, H. Haugan, and G. J. Brown, Phys. Rev. B **69**, 155321 (2004).
[26] C. H. Grein, Private communication (2016).
[27] A.-B. Chen and A. Sher, *Semiconductor Alloys* (Plenum, New York, 1995); Ch. 7.
[28] I. Vurgaftman, J. R. Meyer, and L. R. Ram-Mohan, J. Appl. Phys. **89**, 5815 (2001).
[29] V. Virkkala, V. Havu, F. Tuomisto, and M. J. Puska, Phys. Rev. **86**, 144101 (2012).
[30] J. Heyd, J. E. Peralta, G. E. Scuseria, and R. L. Martin, J. Chem. Phys. **123**, 174101 (2005).
[31] M. H. Hakala and A. S. Foster, *Sci.. and Tech.* [Aalto University Publication Series, Finland] 19, 1 (2013).
[32] S. Krishnamurthy and M. A. Berding, J. of Appl. Phys. **90**(3), 828 (2001).
[33] C. G. Van de Walle, P. H. Denteneer, Y. Bar-Yam, and S. T. Pantelides, Phys. Rev. B **39**, 10791 (1989).
[34] M. A. Berding and A. Sher, Phys. Rev. B **56**, 3885 (1997).
[35] Z.-G. Yu and S. Krishnamurthy, AIP Advances **7**, 065203 (2017).